Strål
säkerhets
myndigheten
Swedish Radiation Safety Authority

Authors: Jeoung Seok Yoon[1], Ove Stephansson[1] and Ki-Bok Min[2]
[1] Stephansson Rock Consultant, Berlin, Germany
[2] Seoul National University, Seoul, South Korea

Technical Note 74; page 143-162

2014:59

Relation between earthquake magnitude, fracture length and fracture shear displacement in the KBS-3 repository at Forsmark

Main Review Phase

Date: December 2014
Report number: 2014:59 **ISSN:** 2000-0456
Available at www.stralsakerhetsmyndigheten.se

Result of all PFC modelling cases

In this appendix, all the figures resulting from 38 modelling cases (see Table 9) are presented.

Models in Section 5.1

Thermal induced, simultaneous heating, present day most likely stress, DFN03h

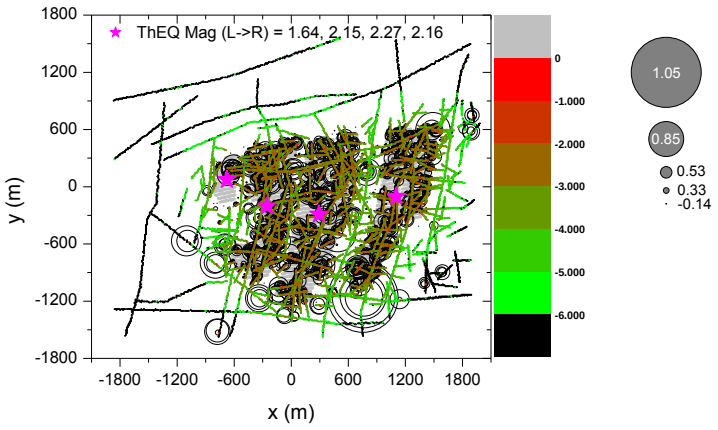

Figure A3-1. Spatial distribution of the induced seismic events and shear displacement of joint planes that constitute the TFs and DZs, due to simultaneous heating and after 25 years with realization DFN03h.

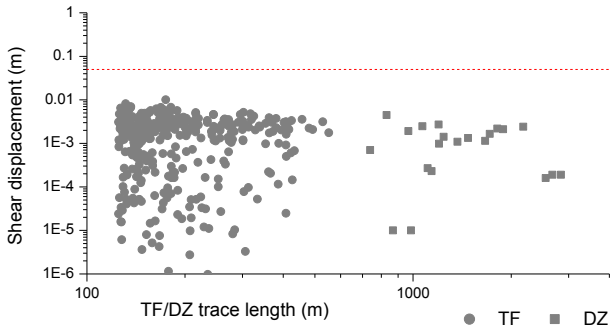

Figure A3-2. Shear displacement of the TFs and DZs with respect to length, due to simultaneous heating and after 25 years with realization DFN03h.

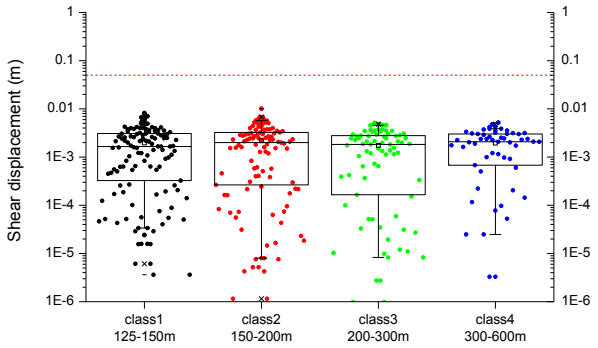

Figure A3-3. Box-and-whisker diagram of the TF shear displacement in four trace length classes, due to simultaneous heating and after 25 years with realization DFN03h.

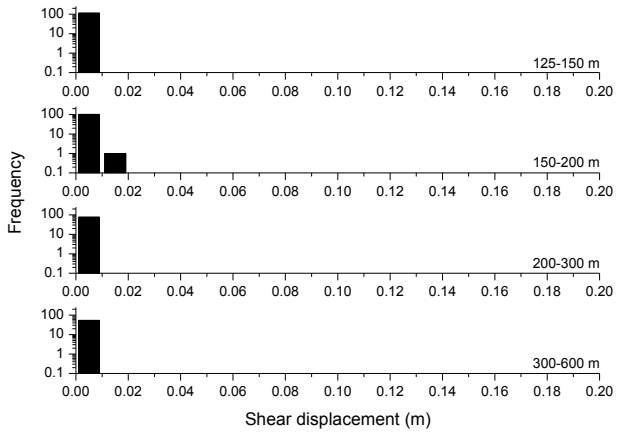

Figure A3-4. Histogram of shear displacement of the TFs in four different trace length classes, due to simultaneous heating and after 25 years with realization DFN03h.

Thermal induced, simultaneous heating, present day most likely stress, DFN06h

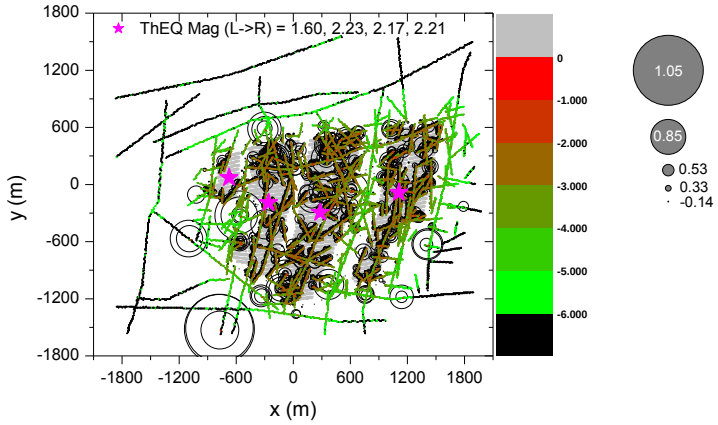

Figure A3-5. Spatial distribution of the induced seismic events and shear displacement of the joint planes that constitute the TFs and DZs, due to simultaneous heating and after 25 years with realization DFN06h.

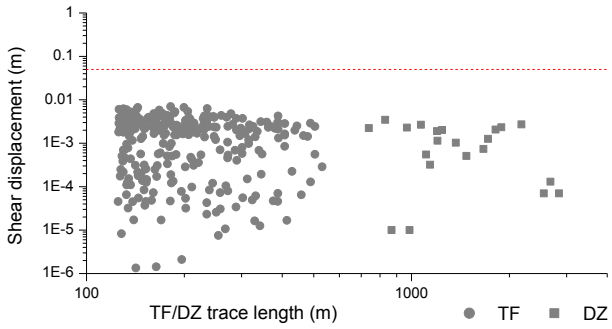

Figure A3-6. Shear displacement of the TFs and DZs with respect to length, due to simultaneous heating and after 25 years with realization DFN06h.

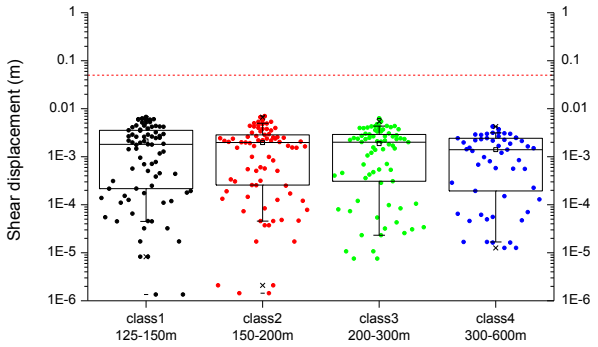

Figure A3-7. Box-and-whisker diagram of the TF shear displacement in four trace length classes, due to simultaneous heating and after 25 years with realization DFN06h.

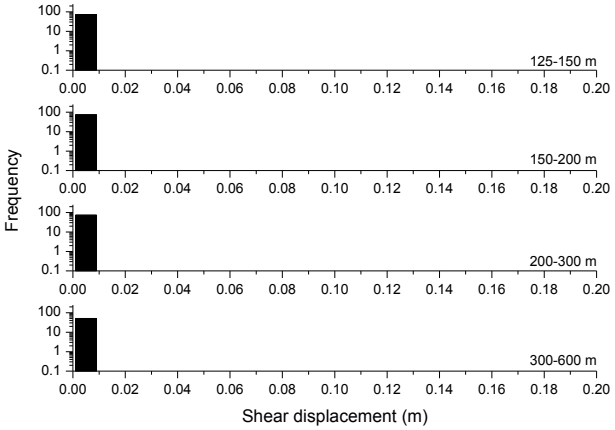

Figure A3-8. Histogram of shear displacement of the TFs in four different trace length classes, due to simultaneous heating and after 25 years with realization DFN06h.

Models in Section 5.2

Thermal induced, sequential heating, present day most likely stress, DFN03h

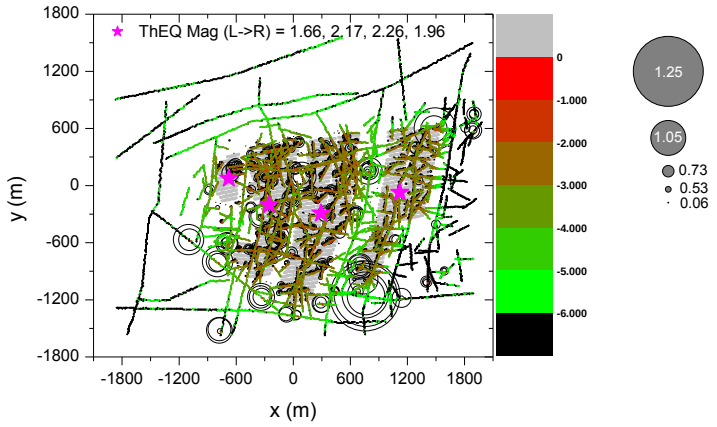

Figure A3-9. Spatial distribution of the induced seismic events and shear displacement of the joint planes of the TFs and DZs, due to sequential heating and after 50 years from start of deposition with realization DFN03h.

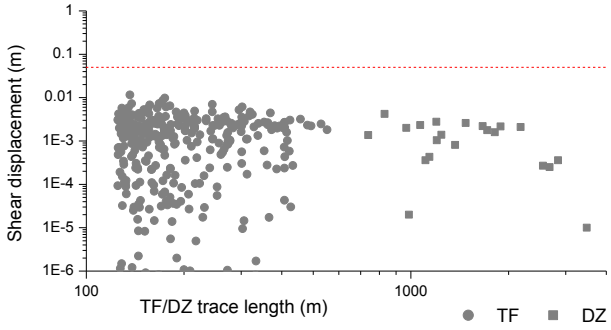

Figure A3-10. Shear displacement of the TFs and DZs with respect to length, due to sequential heating and after 50 years from start of deposition with realization DFN03h.

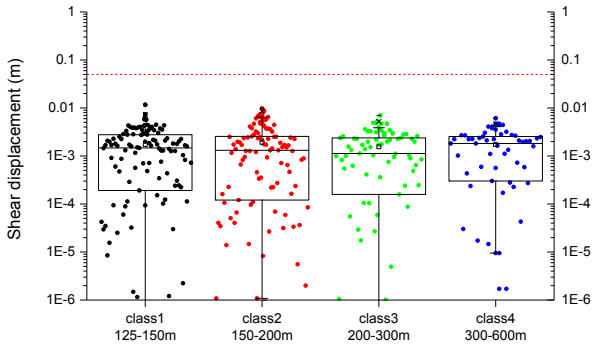

Figure A3-11. Box-and-whisker diagram of the TF shear displacement in four trace length classes, due to sequential heating and after 50 years from start of deposition with realization DFN03h.

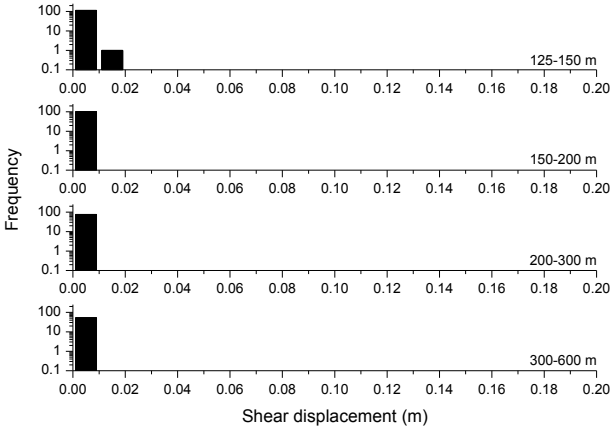

Figure A3-12. Histogram of shear displacement of TFs in four different trace length classes, due to sequential heating and after 50 years from start of deposition with realization DFN03h.

Thermal induced, sequential heating, present day most likely stress, DFN06h

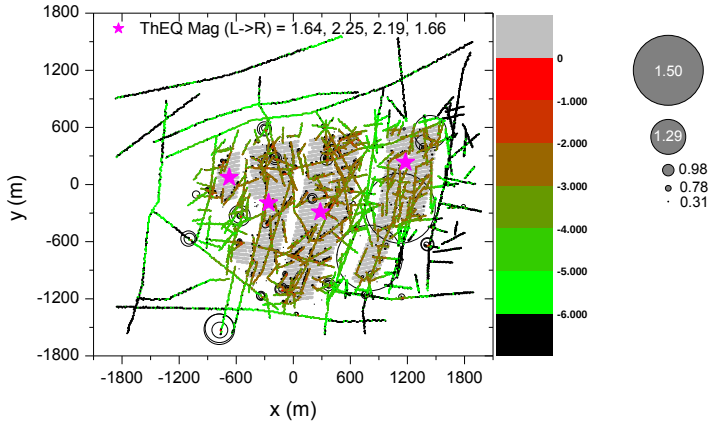

Figure A3-13. Spatial distribution of the induced seismic events and shear displacement of the joint planes of the TFs and DZs, due to sequential heating and after 50 years from start of deposition with realization DFN06h.

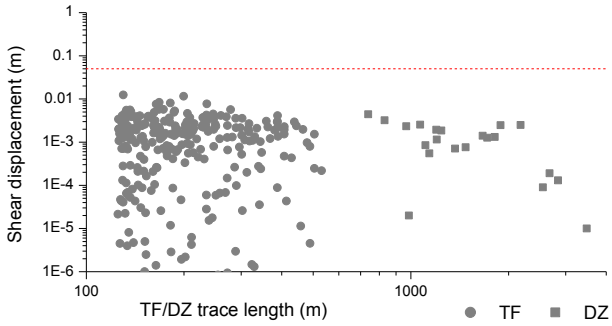

Figure A3-14. Shear displacement of the TFs and DZs with respect to the trace length, due to sequential heating and after 50 years from start of deposition with realization DFN06h.

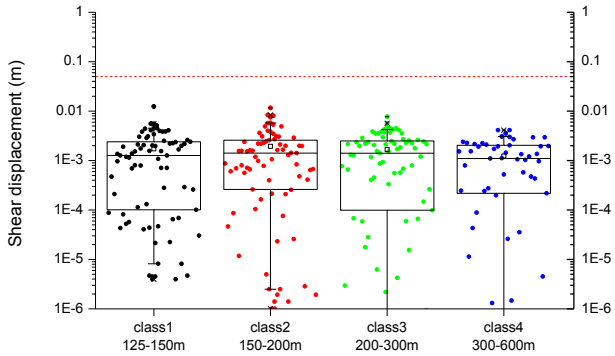

Figure A3-15. Box-and-whisker diagram of the TF shear displacement in four trace length classes, due to sequential heating and after 50 years from start of deposition with realization DFN06h.

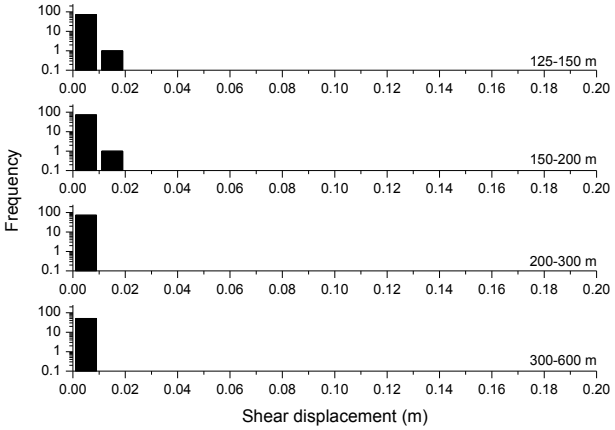

Figure A3-16. Histogram of shear displacement of the TFs in four different trace length classes, due to sequential heating and after 50 years from start of deposition with realization DFN06h.

Models in Section 6.1

Earthquake induced, ZFMWNW0809A, present day most likely stress, DFN03h

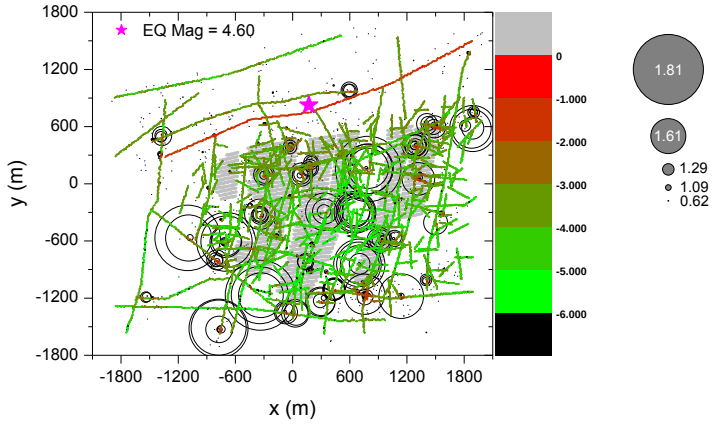

Figure A3-17. Spatial distribution of the induced seismic events and shear displacement of the joint planes that consist the TFs and DZs, due to seismic event at zone ZFMWNW0809A with realization DFN03h.

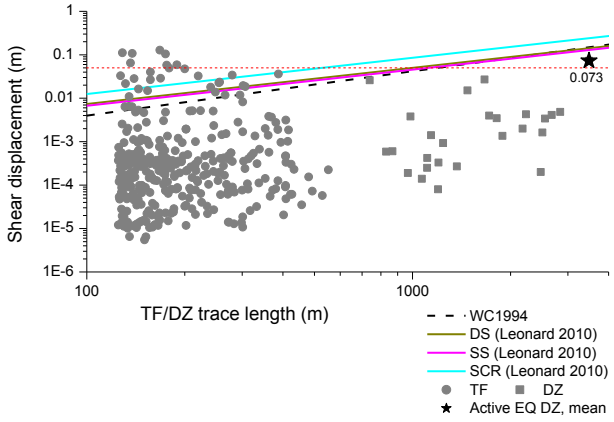

Figure A3-18. Shear displacement of the TFs and DZs with respect to length, due to seismic event at zone ZFMWNW0809A with realization DFN03h and comparison with empirical regressions.

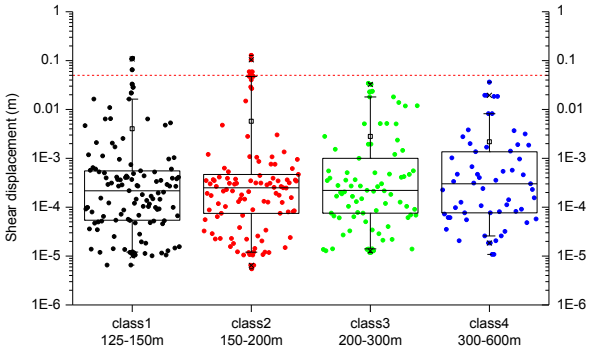

Figure A3-19. Box-and-whisker diagram of the TF shear displacement in four trace length classes, due to seismic event at zone ZFMWNW0809A with realization DFN03h.

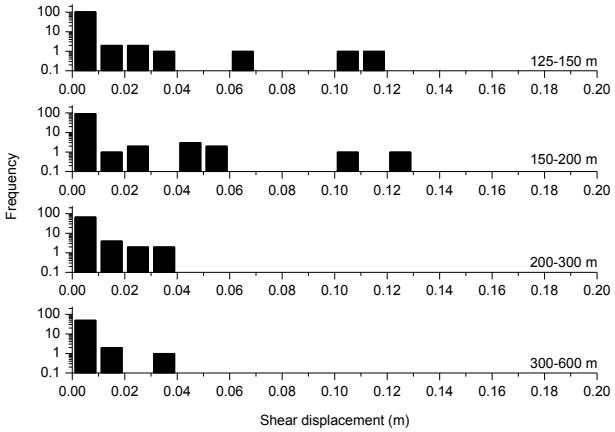

Figure A3-20. Histogram of shear displacement of the TFs in four different trace length classes, due to seismic event at zone ZFMWNW0809A with realization DFN03h.

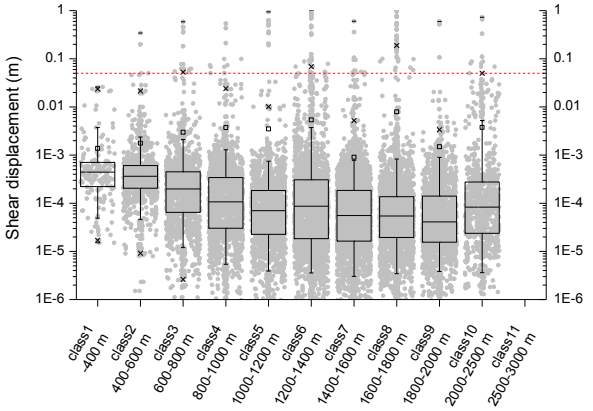

Figure A3-21. Box-and-whisker diagram of shear displacement smooth joints of TFs in nine classes of distance from the hypocentre of simulated earthquake.

Earthquake induced, ZFMWNW0809A, present day most likely stress, DFN06h

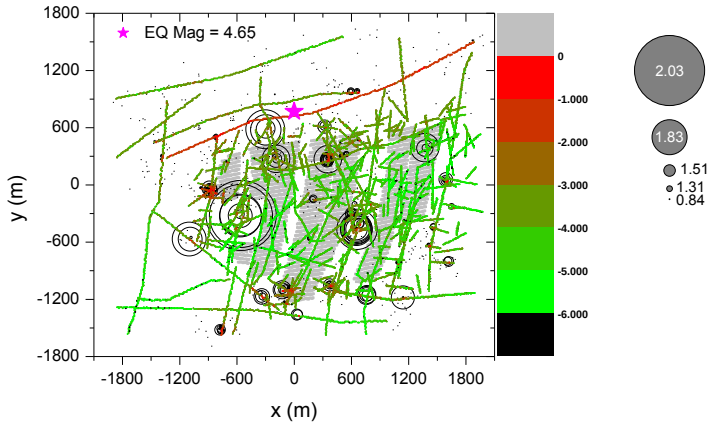

Figure A3-22. Spatial distribution of the induced seismic events and shear displacement of the joint planes that constitute the TFs and DZs, due to seismic event at zone ZFMWNW0809A with realization DFN06h.

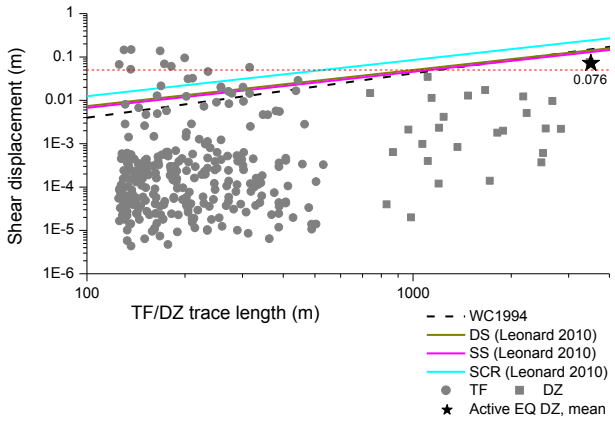

Figure A3-23. Shear displacement of the TFs and DZs with respect to length, due to seismic event at zone ZFMWNW0809A with realization DFN06h and comparison with empirical regressions.

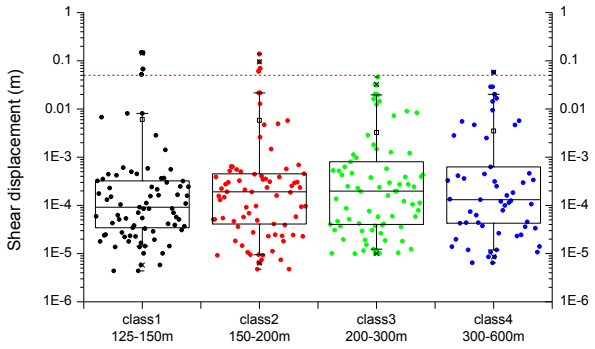

Figure A3-24. Box-and-whisker diagram of the TF shear displacement in four trace length classes, due to seismic event at zone ZFMWNW0809A with realization DFN06h.

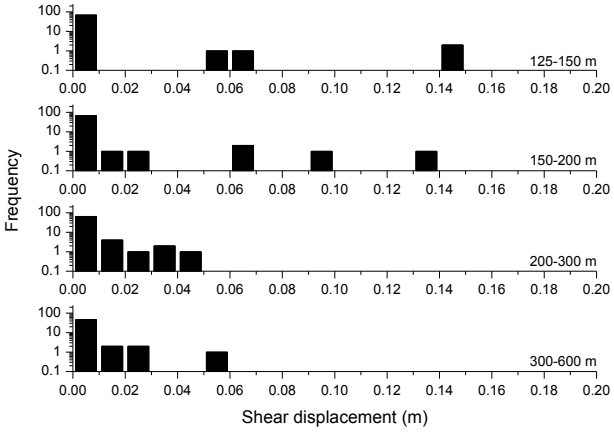

Figure A3-25. Histogram of shear displacement of the TFs in four different trace length classes, due to seismic event at zone ZFMWNW0809A with realization DFN06h.

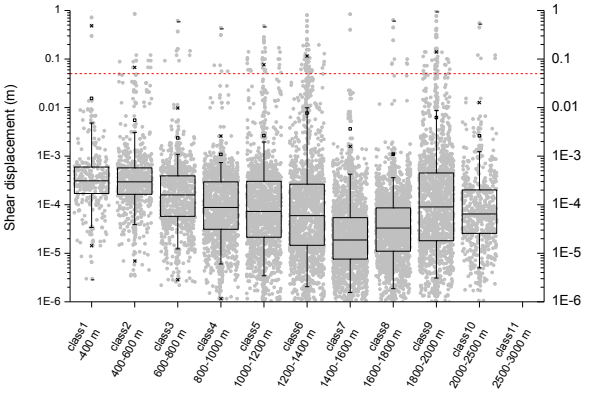

Figure A3-26. Box-and-whisker diagram of shear displacement of the smooth joints of the TFs in nine classes of distance from the hypocentre of simulated earthquake.

Earthquake induced, ZFMWNW0001, present day most likely stress, DFN03h, powered shear force

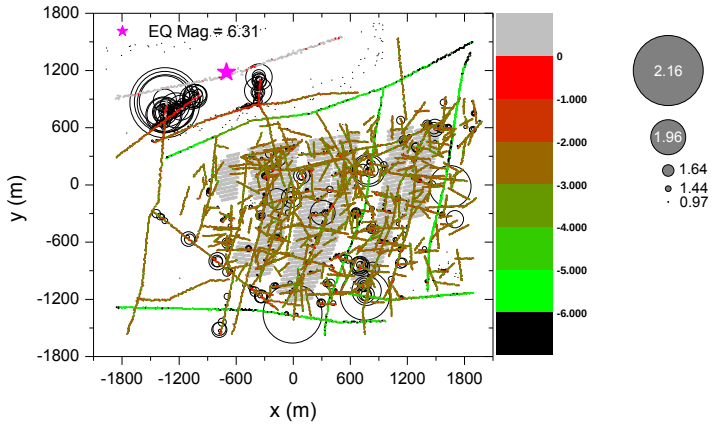

Figure A3-27. Spatial distribution of the induced seismic events and shear displacement of the joint planes that constitute the TFs and DZs, due to seismic event at zone ZFMWNW0001 with realization DFN03h.

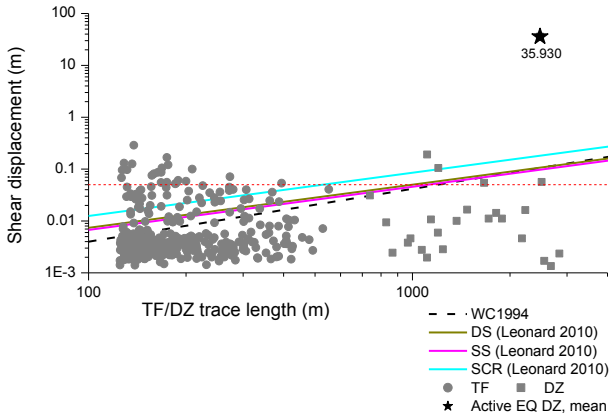

Figure A3-28. Shear displacement of the TFs and DZs with respect to length, due to seismic event at zone ZFMWNW0001 with realization DFN03h and comparison with empirical regressions.

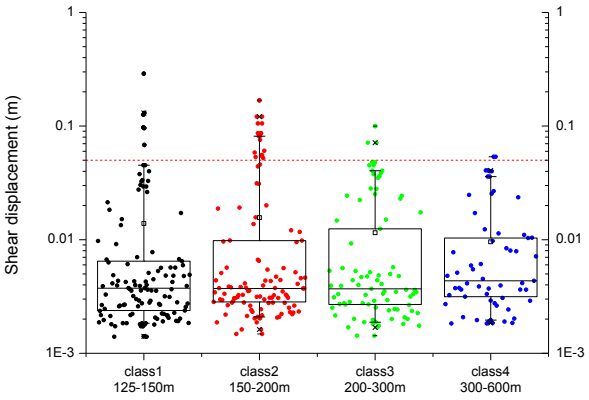

Figure A3-29. Box-and-whisker diagram of the TF shear displacement in four trace length classes, due to seismic event at zone ZFMWNW0001 with realization DFN03h

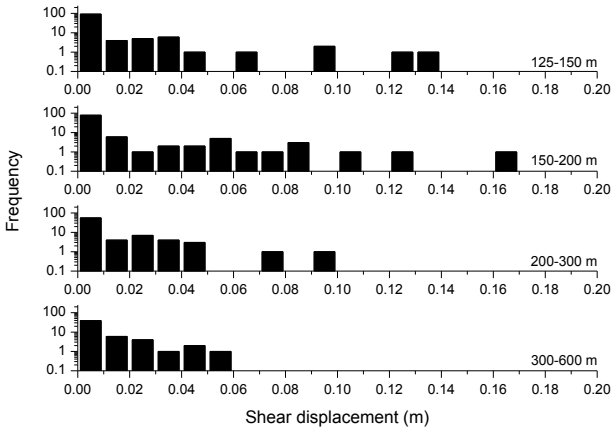

Figure A3-30. Histogram of shear displacement of the TFs in four different trace length classes, due to seismic event at zone ZFMWNW0001 with realization DFN03h.

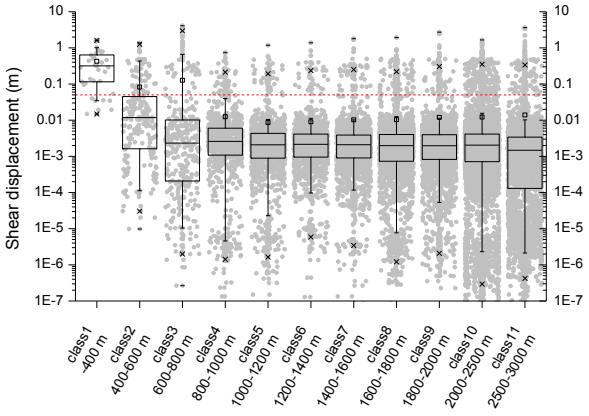

Figure A3-31. Box-and-whisker diagram of shear displacement of the smooth joints of TFs in six classes of distance from the hypocentre of the simulated earthquake.

Earthquake induced, ZFMWNW0001, present day most likely stress, DFN06h, powered shear force

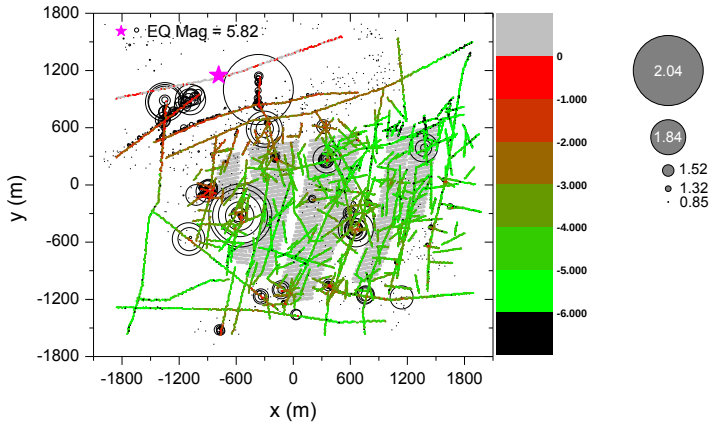

Figure A3-32. Spatial distribution of the induced seismic events and shear displacement of the joint planes that constitute the TFs and DZs, due to seismic event at zone ZFMWNW0001 with realization DFN06h.

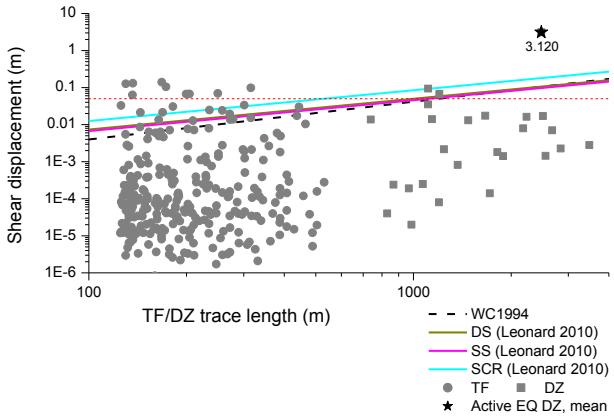

Figure A3-33. Shear displacement of the TFs and DZs with respect to length, due to seismic event at zone ZFMWNW0001 with realization DFN06h and comparison with empirical regressions.

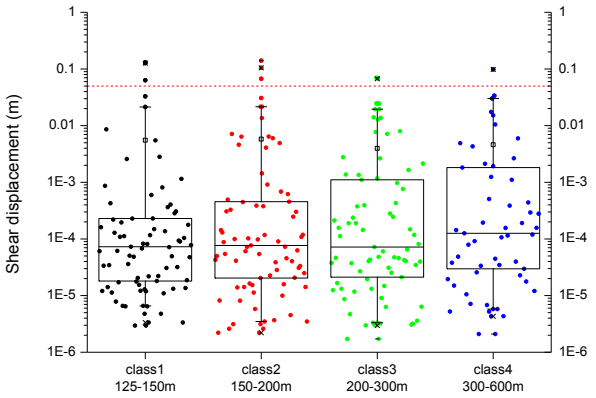

Figure A3-34. Box-and-whisker diagram of the TF shear displacement in four trace length classes, due to seismic event at zone ZFMWNW0001 with realization DFN06h.

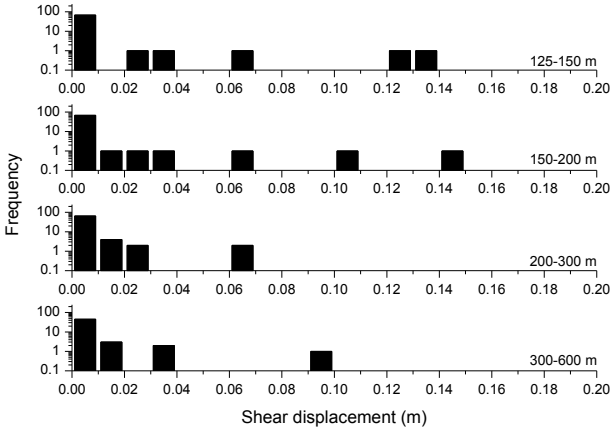

Figure A3-35. Histogram of shear displacement of the TFs in four different trace length classes, due to seismic event at zone ZFMWNW0001 with realization DFN06h.

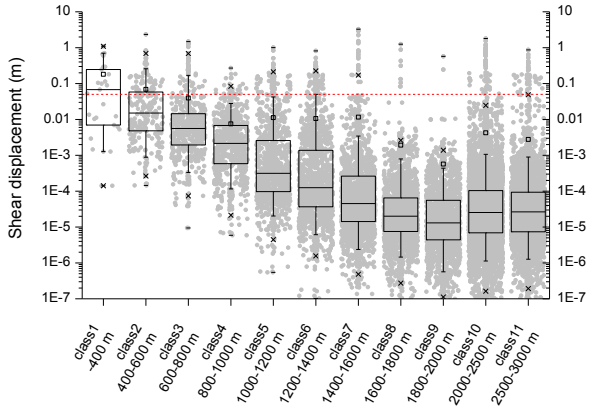

Figure A3-36. Box-and-whisker diagram of the shear displacement of smooth joints of TFs in six classes of distance from the hypocentre of simulated earthquake.

Earthquake induced, ZFMWNW2225, present day most likely stress, DFN03h

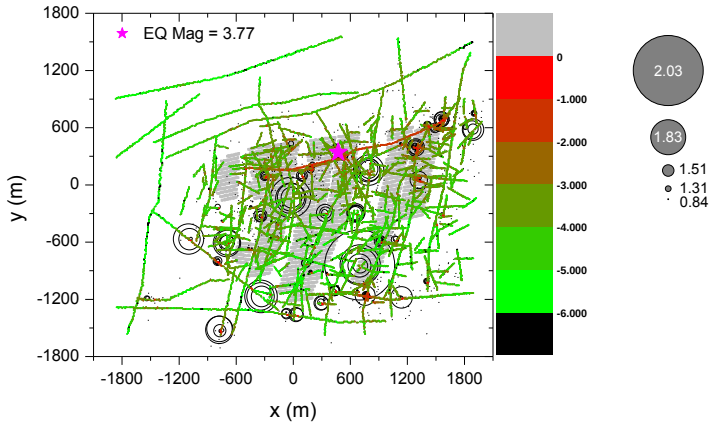

Figure A3-37. Spatial distribution of the induced seismic events and shear displacement of the TFs and DZs, due to seismic event at zone ZFMWNW2225 with realization DFN03h.

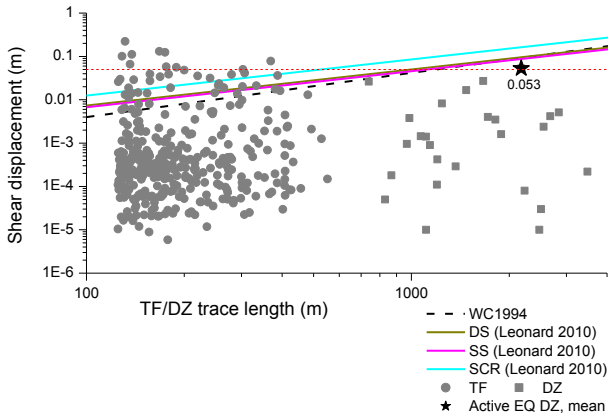

Figure A3-38. Shear displacement of the TFs and DZs with respect to length, due to seismic event at zone ZFMWNW2225 with realization DFN03h and comparison with empirical regressions.

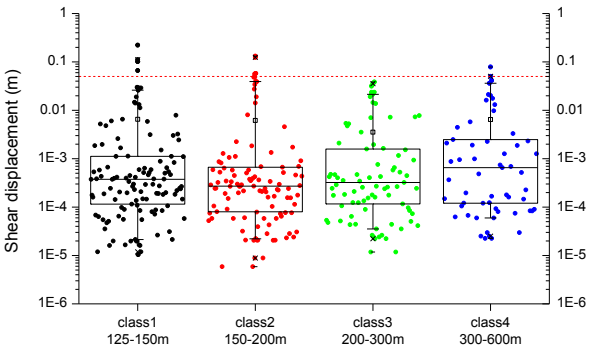

Figure A3-39. Box-and-whisker diagram of the TF shear displacement in four trace length classes, due to seismic event at zone ZFMWNW2225 with realization DFN03h.

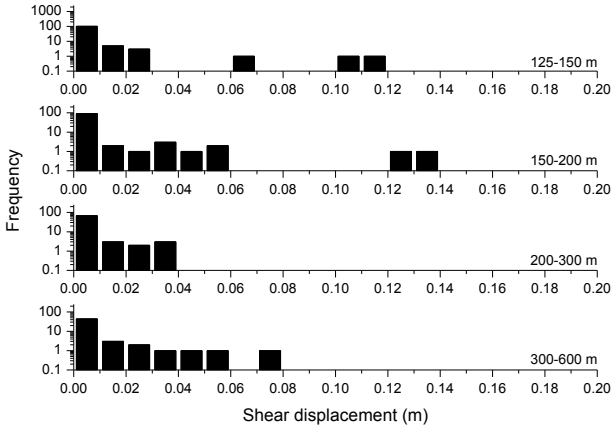

Figure A3-40. Histogram of shear displacement of the TFs in four different trace length classes, due to seismic event at zone ZFMWNW2225 with realization DFN03h.

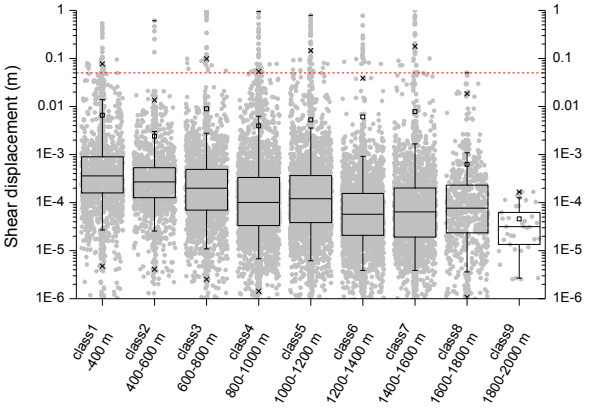

Figure A3-41. Box-and-whisker diagram of the shear displacement of smooth joints of TFs in nine classes of distance from the hypocentre of simulated earthquake.

Earthquake induced, ZFMWNW2225, present day most likely stress, DFN06h

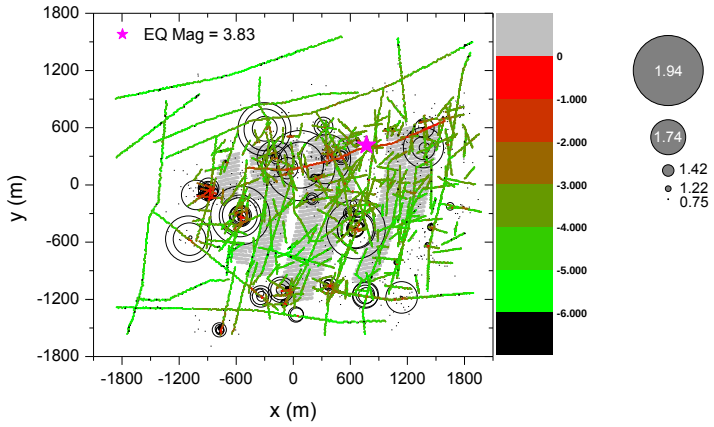

Figure A3-42. Spatial distribution of the induced seismic events and shear displacement of the joint planes that constitute the TFs and DZs, due to seismic event at zone ZFMWNW2225 with realization DFN06h.

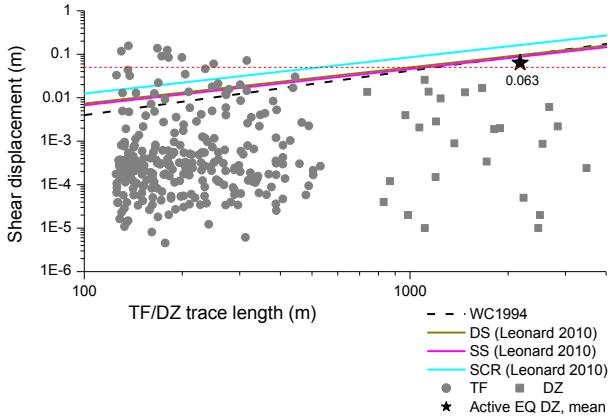

Figure A3-43. Shear displacement of the TFs and DZs with respect to length, due to seismic event at zone ZFMWNW2225 with realization DFN06h and comparison with empirical regressions.

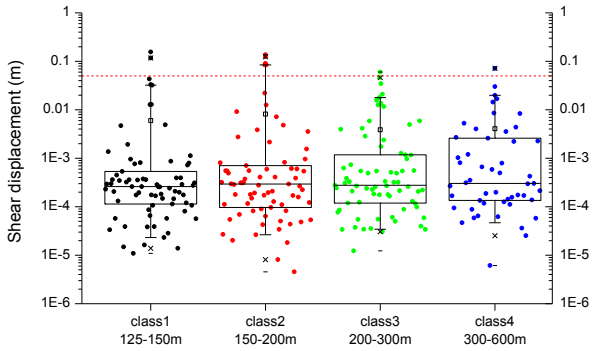

Figure A3-44. Box-and-whisker diagram of the TF shear displacement in four trace length classes, due to seismic event at zone ZFMWNW2225 with realization DFN06h.

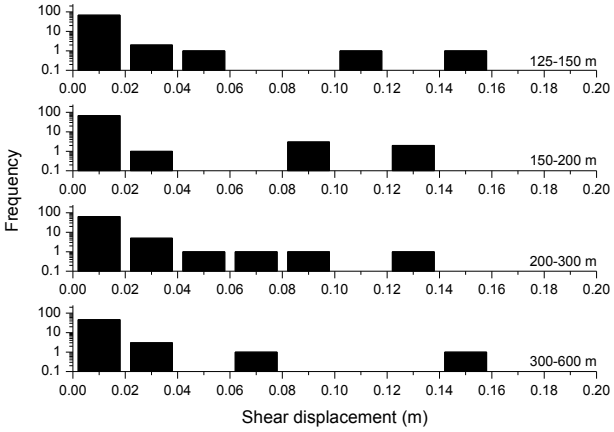

Figure A3-45. Histogram of shear displacement of the TFs in four different trace length classes, due to seismic event at zone ZFMWNW2225 with realization DFN06h.

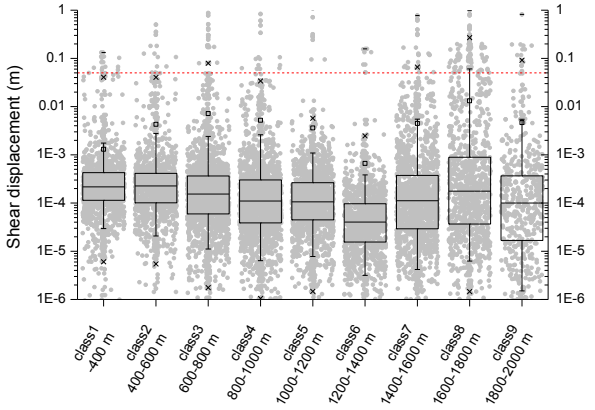

Figure A3-46. Box-and-whisker diagram of the shear displacement of smooth joints of TFs in nine classes of distance from the hypocentre of simulated earthquake.